Influence of Unsteady Aerodynamics on Rotor Blade Aeroelastic Stability and Response

P. P. Friedmann* and L. H. Robinson†
University of California, Los Angeles, Los Angeles, California

This paper describes the incorporation of finite-state, time-domain aerodynamics in a flap-lag-torsional aeroelastic stability and response analysis in forward flight. Improvements to a previous formulation which eliminate spurious singularities are introduced. The methodology for solving the aeroelastic stability and response problems with augmented states, in the time domain, is presented using an implicit formulation. Results illustrating the aeroelastic behavior of soft and stiff in-plane hingeless rotor blades in forward flight are presented to show the sensitivity of both the stability and response problems to time-domain unsteady aerodynamics.

Nomenclature

a_i = incompressible lift-curve slope
A_{21}, A_{22} = coefficients in equations for the augmented states
$\bar{a}\bar{b}R$ = cross-sectional elastic center offset from midchord in Fig. 1
$\bar{b}$ = nondimensional chord, $= b/R$
B_1, B_2, B_3 = coefficients in expressions for Fourier coefficients of H
$\hat{e}_x, \hat{e}_y, \hat{e}_z$ = unit vectors in the undeformed blade coordinate system
$\hat{e}'_x, \hat{e}'_y, \hat{e}'_z$ = the triad $\hat{e}_x, \hat{e}_y, \hat{e}_z$ after deformation
$\hat{e}''_x, \hat{e}''_y, \hat{e}''_z$ = the triad defined by Eq. (7)
e_1 = offset of the blade root from the axis of rotation; $\bar{e}_1 = e_1/\ell$
F = time-domain lift deficiency function
$\Delta h(t)$ = vertical displacement of elastic axis of airfoil
H, H_0, H_{sn}, H_{cn} = a function incorporating unsteady aerodynamic effects and its Fourier coefficients
ℓ = length of elastic portion of blade
L_{nc}, L_c = noncirculatory and circulatory components of lift
M_{nc}, M_c = noncirculatory and circulatory components of moment
$Q(t), \bar{Q}_0, \bar{Q}_{sn}, \bar{Q}_{cn}$ = three-quarter chord downwash velocity and its Fourier coefficients
R = rotor radius
u, v, w = components of displacement of a point on the elastic axis of the blade in the $\hat{e}_x, \hat{e}_y, \hat{e}_z$ directions
U'_x, U'_y, U'_z = velocity vector components in the $\hat{e}'_x, \hat{e}'_y, \hat{e}'_z$ system
U''_x, U''_y, U''_z = velocity vector components in the $\hat{e}''_x, \hat{e}''_y, \hat{e}''_z$ system
$\bar{U}''_{y0}$ = constant portion of $\bar{U}''_y$
$U_T(t), U_p(t)$ = freestream horizontal and vertical velocities in Fig. 1
x_A = aerodynamic center offset from elastic axis
x_0 = radial coordinate along the blade in the $\hat{e}_x$ direction; $\bar{x}_0 = x_0/\ell$
$X_1(t), X_2(t)$ = augmented state variables
$\bar{X}_{10}, \bar{X}_{1sn}, \bar{X}_{1cn}$ = Fourier coefficients of $\bar{X}_1$
$\bar{X}_{20}, \bar{X}_{2sn}, \bar{X}_{2cn}$ = Fourier coefficients of $\bar{X}_2$
$\alpha(t), \alpha_0, \Delta\alpha(t)$ = angle of attack of the airfoil at the elastic center, $= \alpha_0 + \Delta\alpha(t)$
β_p = precone angle
θ_G = total geometric pitch angle
λ = inflow ratio
μ = advance ratio
ρ_A = density of air
ϕ = torsional elastic deformation of the blade
ψ = blade azimuth
Ω = rotor angular speed
$(\bar{\ })$ = nondimensional quantity
$(\ )_{,x}$ = $\partial/\partial x_0$
$(\dot{\ }), (\ddot{\ })$ = $\partial/\partial t$, $\partial^2/\partial t^2$
$(^*), (^{**})$ = $\partial/\partial\psi$, $\partial^2/\partial\psi^2$

Introduction

PREDICTION of unsteady aerodynamic loads in forward flight is an important ingredient in aeroelastic stability and response calculations for rotor blades. Until recently aeroelastic analyses in forward flight have frequently relied on quasisteady, two-dimensional aerodynamics. On the other hand, aeroelastic analyses in hover have been often carried out using frequency domain unsteady aerodynamics.[1,2] This approach was a consequence of the mathematical lack of compatibility between two-dimensional frequency domain theories in the periodic equations of motion that govern blade dynamics in forward flight. Quasisteady theories cannot capture the unsteady effects present at higher frequencies, which may be significant for higher modes in an aeroelastic analysis, or vibratory loads in the presence of a higher harmonic control system.[2]

An attractive alternative to quasisteady aerodynamics is the dynamic inflow model[3,4] that has been used recently in a number of coupled flap-lag-torsional aeroelastic analyses in forward flight.[5-9] This is essentially a low frequency approximation to unsteady aerodynamics in the time domain. Therefore its use for higher frequencies such as vibratory load calculation in the presence of a higher harmonic control system might be questionable.

A generalized version of Greenberg's theory and its finite-state, time-domain approximation have been recently developed by Friedmann and Dinyavari[9-11] and applied to a flap-lag aeroelastic problem of a rotor blade in forward flight. In Ref.

Received Aug. 1988; revision received June 1989.

*Professor and Chairman, Mechanical, Aerospace and Nuclear Engineering Department. Associate Fellow AIAA.

†Doctoral Candidate; currently Dynamics Engineer, McDonald Douglas Helicopter Co., Mesa, Arizona. Student Member AIAA.

10 the unsteady loads on a blade cross section are represented in terms of two additional augmented states, which convey information about the unsteady wake. These augmented states are governed by a first-order system of linear equations, which are driven by the downwash velocity at the airfoil three-quarter chord point. In implementing this theory, a spurious singularity was introduced at high advance ratios.

The present study has a number of objectives:

1) Refinement of the aerodynamic formulation to remove the spurious singularity introduced in Ref. 10 and to produce correct loads at any advance ratio.

2) Extension of finite-state, time-domain unsteady aerodynamics to a flap-lag-torsional aeroelastic analysis through a new implicit method of solution for the augmented states.

3) Calculation of aeroelastic response and stability for soft- and stiff-in-plane hingeless blade configurations using both quasisteady and unsteady aerodynamics to determine the effects of unsteadiness from comparing these two sets of results.

4) Assessment of the influence of unsteady aerodynamics on rotor response in the presence of high-frequency excitations.

Arbitrary-Motion Lift and Moment

The general noncirculatory and circulatory arbitrary-motion airloads on an airfoil, such as that shown in Fig. 1, were derived in Ref. 10 and are given by

$$L_{nc}(t) = \tfrac{1}{2}\rho_A a_i(\bar{b}R)^2\Big\{\Delta\dot{h}(t) + U_T(t)\Delta\dot{\alpha}(t) + \dot{U}_T(t)\big[\alpha_0 + \Delta\alpha(t)\big] - \dot{U}_p(t) - (\bar{a}\bar{b}R)\Delta\ddot{\alpha}(t)\Big\} \quad (1)$$

$$M_{nc}(t) = \underline{\tfrac{1}{2}\rho_A a_i(\bar{b}R)^2 U_T(t)Q(t)} + \tfrac{1}{2}\rho_A a_i(\bar{b}R)^3\Big\{(\bar{a}-\tfrac{1}{2})U_T\Delta\dot{\alpha}(t) + \bar{a}\big[\Delta\dot{h}(t) - \dot{U}_p(t)\big] + \bar{a}\dot{U}_T(t)\big[\alpha_0 + \Delta\alpha(t)\big] - \bar{b}R(\tfrac{1}{8} + \bar{a}^2)\Delta\ddot{\alpha}(t)\Big\} \quad (2)$$

$$L_c(t) = \rho_A a_i(\bar{b}R)U_T(t)\left[0.006825\left(\frac{U_{T0}}{\bar{b}R}\right)^2 X_1(t) + 0.10805\left(\frac{U_{T0}}{\bar{b}R}\right)X_2(t)\right] + \tfrac{1}{2}\rho_A a_i(\bar{b}R)U_T(t)Q(t) \quad (3)$$

$$M_c(t) = \bar{b}R(\bar{a}+\tfrac{1}{2})L_c(t) - \underline{\tfrac{1}{2}\rho_A a_i(\bar{b}R)^2 U_T(t)Q(t)} \quad (4)$$

where the two underlined terms cancel each other, and U_{T0} is the constant portion of U_T. From Fig. 1 it can be seen that the three-quarter chord downwash velocity $Q(t)$ will have contributions due to oncoming velocity $U_T(t)$, vertical velocity $\Delta\dot{h}(t) - U_p(t)$, and angular rotation $\Delta\dot{\alpha}(t)$.

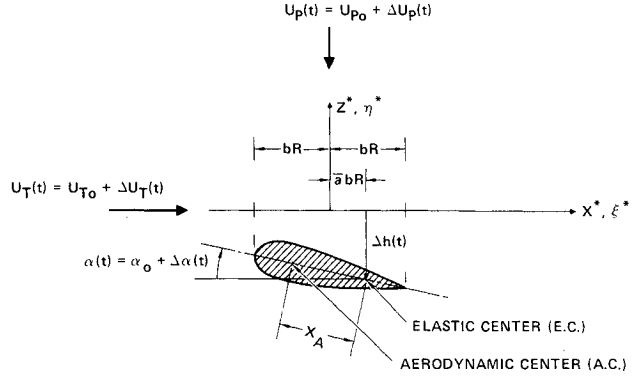

Fig. 1 Geometry of motion of typical airfoil.

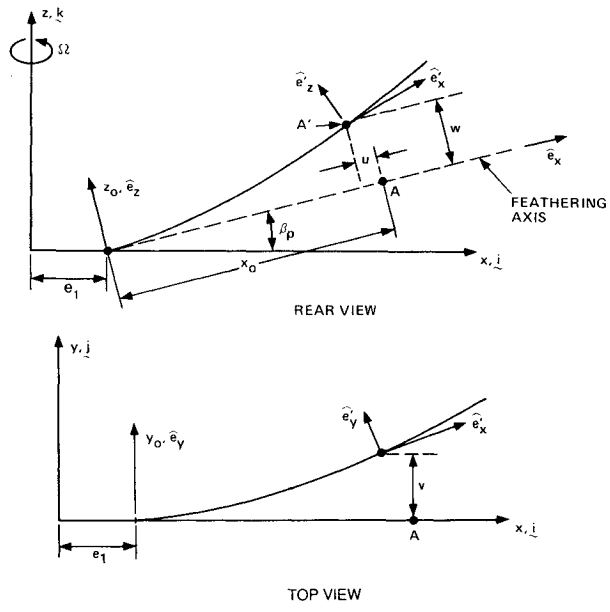

Fig. 2 Geometry of the blade elastic axis before and after deformation.

$$Q(t) = U_T(t)\sin\big[\alpha_0 + \Delta\alpha(t)\big] + \big[\Delta\dot{h}(t) - U_p(t)\big]\cos\big[\alpha_0 + \Delta\alpha(t)\big] + \bar{b}R(\tfrac{1}{2} - \bar{a})\Delta\dot{\alpha}(t) \quad (5)$$

The augmented states X_1 and X_2 are governed by[10]

$$\begin{Bmatrix}\dot{X}_1(t)\\ \dot{X}_2(t)\end{Bmatrix} = \begin{bmatrix}0 & 1\\ -0.01365(U_{T0}/\bar{b}R)^2 & -0.3455(U_{T0}/\bar{b}R)\end{bmatrix} \times \begin{Bmatrix}X_1(t)\\ X_2(t)\end{Bmatrix} + \begin{Bmatrix}0\\ Q(t)\end{Bmatrix} \quad (6)$$

It is worthwhile mentioning that due to the implicit formulation of the aerodynamic loads, the small angle assumption, usually made in Eq. (5), can be deleted. On one hand, the unsteady aerodynamic theory[10] is essentially linear since it is based on the linear small disturbance, unsteady, perturbation potential equation. On the other hand, the retention of geometrically nonlinear terms in the aeroelastic problem formulation requires a careful treatment when approximating sines and cosines by the small angle approximation. This represents a basic, inherent inconsistency, which is present when dealing with geometrically nonlinear aeroelastic formulations commonly used in rotary-wing aeroelasticity. In such formulations the structural and inertia operators are accurate since they contain geometric nonlinearities consistently, whereas the accuracy of aerodynamic expressions is limited by the linear nature of the aerodynamic theories employed.

Lift and Moment in Terms of Local Blade Velocities

The geometry of the blade before and after deformation is shown in Figs. 2 and 3. To apply Eqs. (1-4) to the present problem, it is convenient to consider, as was done in Ref. 12, a system of unit vectors $\hat{e}_x'', \hat{e}_y'', \hat{e}_z''$, where the double primed system has been rotated by an angle of $-\phi\hat{e}_x'$ from the deformed blade coordinate system, i.e.,

$$\begin{Bmatrix}\hat{e}_y''\\ \hat{e}_z''\end{Bmatrix} = \begin{bmatrix}\cos\phi & -\sin\phi\\ \sin\phi & \cos\phi\end{bmatrix}\begin{Bmatrix}\hat{e}_y'\\ \hat{e}_z'\end{Bmatrix} \quad (7)$$

The velocities in the two systems are therefore related by

$$U_y'' = U_y' - \phi U_z'; \qquad U_z'' = \phi U_y' + U_z' \quad (8)$$

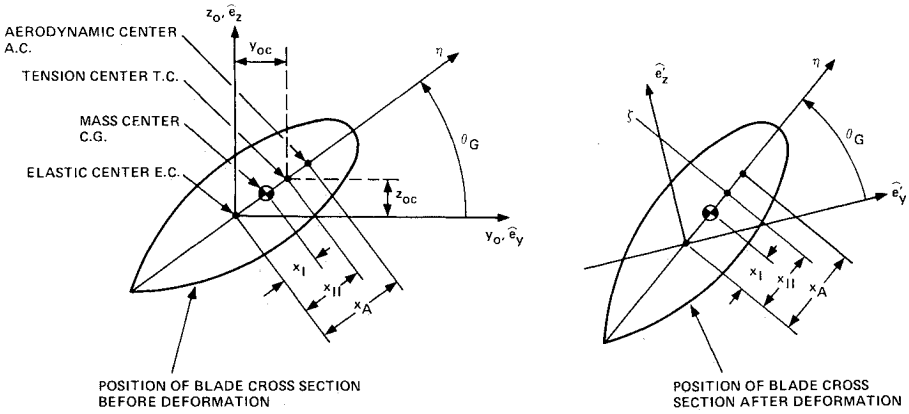

Fig. 3 Blade cross sectional geometry.

The velocities used in this derivation will be velocities of the elastic axis, as were used in Ref. 10, rather than velocities relative to the elastic axis, as were used in Ref. 12. With this convention, the following relations can be identified:

$$U_T = U_y''; \qquad \alpha_0 + \Delta\alpha = \theta_G + \phi; \qquad U_p - \Delta\dot{h} = U_z'' \tag{9}$$

Substituting the preceding velocity terms in Eqs. (1-4) and using the following notation

$$\frac{\partial}{\partial t} = \Omega\frac{\partial}{\partial\psi}, \quad \bar{x}_A = \frac{x_A}{\bar{b}R}, \quad \bar{a} = (\bar{x}_A - \tfrac{1}{2}), \quad \overline{R} = \frac{R}{\ell}$$

$$\overline{U}_y = \frac{U_y}{\Omega\ell}, \quad \overline{U}_z = \frac{U_z}{\Omega\ell}, \quad \overline{X}_1 = \frac{\Omega}{\ell}X_1, \quad \overline{X}_2 = \frac{X_2}{\ell}$$

$$\overline{L}_{nc} = \frac{L_{nc}}{a_i\rho_A(\bar{b}R)(\Omega\ell)^2}, \qquad \overline{M}_{nc} = \frac{M_{nc}}{a_i\rho_A(\bar{b}R)^2(\Omega\ell)^2}$$

$$\overline{L}_c = \frac{L_c}{a_i\rho_A(\bar{b}R)(\Omega\ell)^2}, \qquad \overline{M}_c = \frac{M_c}{a_i\rho_A(\bar{b}R)^2(\Omega\ell)^2} \tag{10}$$

the noncirculatory lift and moment become

$$\overline{L}_{nc} = \frac{\overline{bR}}{2}\left\{\overline{U}_y''(\overset{*}{\theta}_G + \overset{*}{\phi}) - \overset{*}{\overline{U}}_z'' - \overline{bR}(\bar{x}_A - \tfrac{1}{2})(\overset{**}{\theta}_G + \overset{**}{\phi}) + \overset{*}{\overline{U}}_y''(\theta_G + \phi)\right\} \tag{11}$$

$$\overline{M}_{nc} = \frac{\overline{bR}}{2}\left\{(\bar{x}_A - 1)\overline{U}_y''(\overset{*}{\theta}_G + \overset{*}{\phi}) - (\bar{x}_A - \tfrac{1}{2})\overset{*}{\overline{U}}_z'' + (\bar{x}_A - \tfrac{1}{2})\overset{*}{\overline{U}}_y''(\theta_G + \phi) - \overline{bR}(3/8 + \bar{x}_A^2 - \bar{x}_A)(\overset{**}{\theta}_G + \overset{**}{\phi})\right\} \tag{12}$$

the three-quarter chord downwash velocity becomes

$$\overline{Q}(t) = \frac{Q(t)}{\Omega\ell} = \overline{U}_y''\sin(\theta_G + \phi) - \overline{U}_z''\cos(\theta_G + \phi) + \overline{bR}(1 - \bar{x}_A)(\overset{*}{\theta}_G + \overset{*}{\phi}) \tag{13}$$

and the circulatory lift and moment become

$$\overline{L}_c = \overline{U}_y''\left[0.006825\left(\frac{\overline{U}_{y0}''}{\overline{bR}}\right)^2\overline{X}_1(\psi) + 0.10805\left(\frac{\overline{U}_{y0}''}{\overline{bR}}\right)\overline{X}_2(\psi)\right] + \tfrac{1}{2}\overline{U}_y''\overline{Q} \tag{14}$$

$$\overline{M}_c = \bar{x}_A\overline{L}_c \tag{15}$$

where the nondimensional augmented states are now governed by

$$\begin{Bmatrix}\overset{*}{\overline{X}}_1\\ \overset{*}{\overline{X}}_2\end{Bmatrix} = \begin{bmatrix}0 & 1\\ A_{21} & A_{22}\end{bmatrix}\begin{Bmatrix}\overline{X}_1\\ \overline{X}_2\end{Bmatrix} + \begin{Bmatrix}0\\ \overline{Q}\end{Bmatrix} \tag{16}$$

where

$$A_{21} = -0.01365\left(\frac{\overline{U}_{y0}''}{\overline{bR}}\right)^2; \qquad A_{22} = -0.3455\left(\frac{\overline{U}_{y0}''}{\overline{bR}}\right) \tag{17}$$

The circulatory lift can be written in a more convenient form if a quantiy incorporating unsteady effects is defined as

$$H = \left[0.006825\left(\frac{\overline{U}_{y0}''}{\overline{bR}}\right)^2\overline{X}_1(\psi) + 0.10805\left(\frac{\overline{U}_{y0}''}{\overline{bR}}\right)\overline{X}_2(\psi)\right] \tag{18}$$

then the circulatory lift can be written as

$$\overline{L}_c = \overline{U}_y''\left[H + \tfrac{1}{2}\overline{Q}\right] \tag{19}$$

Previous Formulation of the Circulatory Lift and Moment

In Ref. 10 the circulatory lift and moment were expressed in terms of a time-dependent lift deficiency function F representing the ratio of time varying lift to quasisteady lift, as

$$\overline{L}_c = [\tfrac{1}{2} + F]\overline{U}_y''\overline{Q}; \qquad \overline{M}_c = \bar{x}_A[\tfrac{1}{2} + F]\overline{U}_y''\overline{Q} \tag{20}$$

where F was defined by

$$F(\overline{X}_{TS1}, \overline{X}_{TS2}, \overline{Q}_{TS}) = \frac{\left[0.006825\left(\frac{\overline{U}_{TS0}}{\overline{bR}}\right)^2\right]\overline{X}_{TS1} + \left[0.10805\left(\frac{\overline{U}_{TS0}}{\overline{bR}}\right)\right]\overline{X}_{TS2}}{\overline{Q}_{TS}} \tag{21}$$

The quantity F was calculated using the augmented states at a typical section (hence the TS subscripts in the expression for F), and thus it was a function of time only. The purpose of this particular formulation was to simplify the solution of the aeroelastic response and stability problem by having the augmented states governing the unsteady aerodynamics be only time-dependent functions that did not change with the location of the blade cross section along the span. Unfortunately this simplified formulation introduced a spurious singularity in the circulatory loads at high advance ratios. For typical rotor blades, the three-quarter chord downwash velocity $\overline{Q}$ can become zero on the advancing side of the rotor at sufficiently high advance ratios. From Eq. (21) it can be seen that when $\overline{Q}_{TS}$ approaches zero, the lift deficiency function F will ap-

proach infinity. When the circulatory lift is evaluated at the typical section, this causes no problem because according to Eq. (20), F is multiplied by $\overline{Q}$, which cancels with the denominator in Eq. (21). If the circulatory lift is calculated at any other location except the typical section, $\overline{Q}$ and $\overline{Q}_{TS}$ do not cancel and as $\overline{Q}_{TS}$ approaches zero, the circulatory lift approaches infinity.

In the present study, this singularity is avoided by allowing the augmented states to vary with spanwise station. The circulatory lift and moment at a point are calculated using the augmented states determined from the time history of the blade at that same point, and thus the singularity encountered in the previous formulation is avoided.

Incorporation of Time Domain Aerodynamics in the Aeroelastic Analysis

The geometry of a hingeless blade undergoing moderate deflections is described by Figs. 2 and 3. The coupled flap-lag-torsional equations of motion are simlar to those derived in Refs. 12 and 13. They form the basis of an implicit, coupled, flap-lag-torsional analysis described recently by Celi and Friedmann.[14] These equations describe the coupled flap-lag-torsional dynamics of a flexible, isotropic, blade, modeled as an Euler-Bernoulli beam underoging small strains and moderate deflections. Thus the equations contain geometrically nonlinear terms in the structural, inertia, and aerodynamic operators associated with this aeroelastic problem. The inertia loads are determined by using D'Alembert's principle.

The unsteady aerodynamic loads are incorporated in the flap-lag-torsional equations following the approach used in Ref. 12. The implicit nature of the implementation eliminates the need for the use of an ordering scheme, and so in this study most higher-order terms were retained in the aerodynamic expressions. Stall and compressibility effects were not included; however these too can be accommodated with the implicit formulation.

The lift and moment quantities in Eqs. (11–15) are in terms of local velocities in the double primed coordinate system of Eq. (7). Expressions for these velocities in terms of blade slopes and displacements are required. In Ref. 12 expressions for V_{EA}, the velocity of the elastic axis, and V_A, the velocity of airflow due to inflow, are found in the single primed deformed coordinate system. When higher-order terms are included, the velocity terms are as follows.

$$
\begin{aligned}
V_{EA} = \Omega\Big[& \left(v_{,x}(\mathring{v}+u+x_0+e_1-w\beta_p)+v(w_{,x}\beta_p-1)\right. \\
& \left.+(w_{,x}\mathring{w}+\mathring{u})(1+\beta_p^2)\right]\hat{e}'_x+\Omega\Big[(\mathring{v}+u+x_0+e_1-w\beta_p) \\
& +\left\{-v_{,x}\mathring{u}+\phi(\mathring{w}-w_{,x}\mathring{u})\right\}(1+\beta_p^2) \\
& +v\left\{\phi(w_{,x}+\beta_p)+v_{,x}\right\}\Big]\hat{e}'_y+\Omega\Big[(1+\beta_p^2)\left\{\mathring{w}+\mathring{u}(\phi v_{,x}-w_{,x})\right\} \\
& -(\phi+v_{,x}w_{,x})(\mathring{v}+u+x_0+e_1-w\beta_p) \\
& +v(w_{,x}+\beta_p-\phi v_{,x})\Big]\hat{e}'_z \qquad (22)
\end{aligned}
$$

$$
\begin{aligned}
V_A = {} & \Omega R\left[\mu\cos\psi+\mu v_{,x}\sin\phi\right]\hat{e}'_x \\
& +\Omega R\left[-\mu v_{,x}\cos\psi-\mu\sin\psi\right]\hat{e}'_y \\
& +\Omega R\Big[-\mu\cos\psi(v_{,x}-\psi v_{,x}+\beta_p) \\
& +\mu\sin\psi(\phi+v_{,x}w_{,x})-\lambda\Big]\hat{e}'_z \qquad (23)
\end{aligned}
$$

From these velocities the total velocity of the elastic axis relative to the air can be found as

$$U = V_{EA} - V_A = U'_x\hat{e}'_x + U'_y\hat{e}'_y + U'_z\hat{e}'_z \qquad (24)$$

Given these velocities in the single-primed system, the velocities in the double-primed system can be found by using Eq. (8).

In actual implementation the axial displacement term u and its time derivatives are neglected. This is inconsistent with retaining all other higher-order terms and is only done because expressions for u and $\mathring{u}$ are not available in the aerodynamic portion of the program. Furthermore, the small angle assumption was made for β_p, which had no effect on calculations since nonzero precone was never used. Air loads are integrated using Gaussian quadrature. Augmented states are therefore needed for each Gaussian point along the blade radius and at numerous equally spaced azimuth locations. This information is stored in the form of Fourier coefficients of the augmented states, which need be calculated only once for each radial station. The augmented states can be determined at any desired value of the azimuth from these coefficients. Additional information on this aspect of the aerodynamic loads is presented in a following section.

Provisions for High-Frequency Pitch Excitation

In order to assess the influence of unsteady aerodynamics on blade response in the presence of high-frequency excitations, sinusoidal root pitch excitations were also included in the appropriate expressions. These excitations may be introduced in the collective, lateral, or longitudinal control degrees of freedom. The excitation may in general be of any amplitude and phasing and may be any integer multiple of the rotor frequency.

To give an indication of the difference in response of the rotor using quasisteady vs unsteady aerodynamics calculations were made to determine the 4/rev components of the in-plane and out-of-plane hub shears for the four bladed rotor. These calculations consisted of integrating the inertia and aerodynamic loads along the blade from the tip to the root then adding up the contributions in the fixed hub coordinate system due to the four rotor blades. For a given response solution in terms of the rotating modes of the blade, these calculations were made at large numbers of equally spaced azimuths, and a Fourier analysis was used to determine the 4/rev components of the hub shears.

Method of Solution

The spatial dependence in the equations of motion is eliminated by using a Galerkin-type, finite-element method.[13,14] A modal coordinate transformation, using the six lowest rotating coupled modes, is performed to reduce the number of degrees of freedom. These modes are calculated at a fixed pitch dependent only on advance ratio. For the configurations considered, the six lowest modes are usually the first three-flap, first two lead-lag, and first torsional modes. The ordinary differential equations are solved using quasilinearization in an iterative manner to obtain the periodic equilibrium position in forward flight for a propulsive trim-type flight condition.[1,14]

An implicit formulation for the aerodynamic loads is used. At each iteration an approximation to the blade response is produced. This response is then used to generate numerical values of the modeling quantities needed in expressions for the aerodynamic loads to be used in the next iteration. Derivatives of the aerodynamic loads with respect to the generalized coordinates, required for stability analysis, are computed using finite difference approximations.[14]

The equations are linearized by writing perturbation equations about the nonlinear equilibrium position. Stability is obtained using Floquet theory.

In the flap-lag analysis of Ref. 10, the two augmented states $\overline{X}_1$ and $\overline{X}_2$ were appended to the state vector for the first-order, state-variable form of the nonlinear periodic equations of motion. The nonlinear equilibrium position was obtained using quasilinearization, and the stability was determined by linearizing about the equilibrium position and applying Floquet theory.

With the implicit formulation of the aerodynamics used in this study, explicit state variables representing the augmented states are not required. Thus the implicit approach offers a significant benefit since the air loads at each point are based on augmented states determined at that point, and so appending augmented states to the system state vector for each point at which air loads are calculated would lead to a problem of untractably large order.

At any radial station for which augmented states are needed, a Fourier analysis of the three-quarter chord downwash velocity (due to the last iteration step used in quasilinearization) is performed. Since the augmented states are driven by the downwash velocity, this yields a Fourier series solution for the augmented states. Subsequently this series solution is then used to obtain the unsteady air loads for the current iteration step of quasilinearization. This procedure converges rapidly to the desired unsteady air loads.

The augmented states at each point are calculated from the time history of $\bar{Q}$ at that point due to the last iteration of quasilinearization. A Fourier analysis may be applied to the time history of $\bar{Q}$ from the last iteration of quasilinearization; thus $\bar{Q}$ is expressed as

$$\bar{Q} = \bar{Q}_0 + \sum_{n=1}^{NH} \left[\bar{Q}_{sn} \sin n\psi + \bar{Q}_{cn} \cos n\psi\right] \tag{25}$$

where NH is the number of harmonics retained in the Fourier analysis. The $\bar{X}_1$ and $\bar{X}_2$ may then be solved for in terms of their Fourier coefficients.

$$\bar{X}_1 = \bar{X}_{10} + \sum_{n=1}^{NH} \left[\bar{X}_{1sn} \sin n\psi + \bar{X}_{1cn} \cos n\psi\right] \tag{26}$$

$$\bar{X}_2 = \bar{X}_{20} + \sum_{n=1}^{NH} \left[\bar{X}_{2sn} \sin n\psi + \bar{X}_{2cn} \cos n\psi\right] \tag{27}$$

Substituting Eqs. (25-27) in Eq. (16) and equating coefficients of sine and cosine leads to the following solution for the Fourier coefficients of the augmented states $\bar{X}_1$ and $\bar{X}_2$

$$\bar{X}_{10} = \frac{-\bar{Q}_0}{A_{21}}, \qquad \bar{X}_{20} = 0$$

$$\bar{X}_{1sn} = \frac{-(A_{21}+n^2)\bar{Q}_{sn} - nA_{22}\bar{Q}_{cn}}{(A_{21}+n^2)^2 + n^2A_{22}^2}$$

$$\bar{X}_{1cn} = \frac{nA_{22}\bar{Q}_{sn} - (A_{21}+n^2)\bar{Q}_{cn}}{(A_{21}+n^2)^2 + n^2A_{22}^2}$$

$$\bar{X}_{2sn} = -n\bar{X}_{1cn}, \qquad \bar{X}_{2cn} = n\bar{X}_{1sn} \tag{28}$$

If Eq. (17) is substituted in Eq. (18), an expression for H in terms of A_{21} and A_{22} can be found.

$$H = -\frac{1}{2}A_{21}\bar{X}_1 - \frac{2162}{6910}A_{22}\bar{X}_2 \tag{29}$$

Furthermore, H is also assumed to have a Fourier series representation.

$$H = H_0 + \sum_{n=1}^{NH} \left[H_{sn} \sin n\psi + H_{cn} \cos n\psi\right] \tag{30}$$

If Eqs. (26-28) are substituted in Eq. (29), then comparison with Eq. (30) yields the following Fourier coefficients for H

$$H_0 = \frac{\bar{Q}_0}{2} \tag{31}$$

$$H_{cn} = \left[\frac{B_1}{B_3}\right]\bar{Q}_{sn} + \left[\frac{B_2}{B_3}\right]\bar{Q}_{cn} \tag{32}$$

$$H_{sn} = \left[\frac{B_2}{B_3}\right]\bar{Q}_{sn} + \left[\frac{-B_1}{B_3}\right]\bar{Q}_{cn} \tag{33}$$

where the following notation is used

$$B_1 = -1294A_{21}A_{22}n + 2162A_{22}n^3$$

$$B_2 = 3455A_{21}(A_{21}+n^2) + 2162A_{22}^2n^2$$

$$B_3 = 6910\left[(A_{21}+n^2)^2 + n^2A_{22}^2\right]$$

The expression for H may be evaluated for any blade radial station and azimuth. Typically five sine and five cosine harmonics are retained in the actual analysis.

Results

In this study a soft-in-plane and a stiff-in-plane hingeless uniform blade baseline configuration, identical to those of Ref. 14, were used. These blades had respectively uncoupled fundamental lag frequencies of 0.732/rev and 1.42/rev and uncoupled fundamental flap and torsion frequencies of 1.125/rev and 3.17/rev. The Lock number was $\gamma = 5.5$, the rotor solidity was $\sigma = 0.07$, and the helicopter weight coefficient was $C_w = 0.005$. The blade root offset e_1 and the precone β_p were zero. The blade was modeled using five finite elements. The procedure used to determine trim values was the same as that employed in Ref. 15. Unless otherwise stated, the results in this paper refer to these baseline configurations.

The blade used in the simplified flap-lag study of Ref. 10 had the same characteristics as the baseline soft-in-plane blade except for the torsional degree of freedom, which was suppressed in Ref. 10. To compare our results with those of Ref. 10, a torsionally stiff blade configuration was used with a relatively high uncoupled fundamental torsional frequency of 6.35/rev. Response and stability calculations were done for the

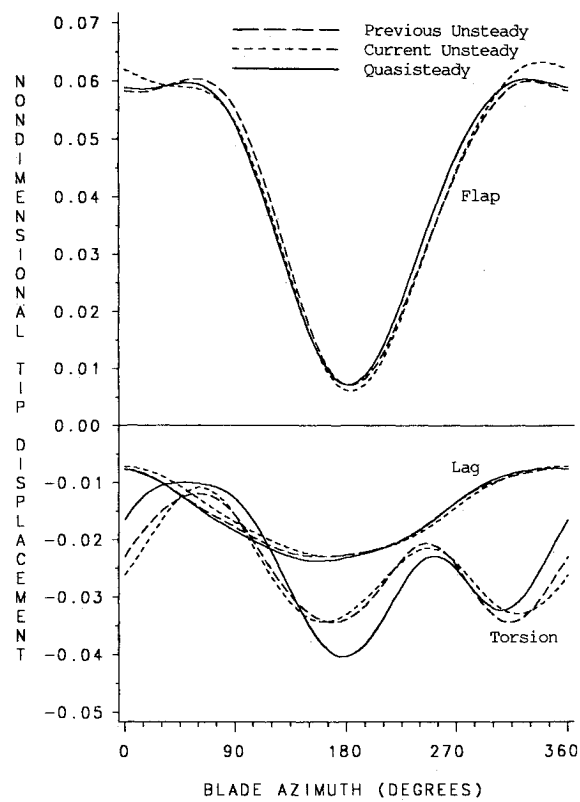

Fig. 4 Blade tip response for quasisteady, previous unsteady, and current unsteady aerodynamic formulation, soft-in-plane blade, advance ratio = 0.4.

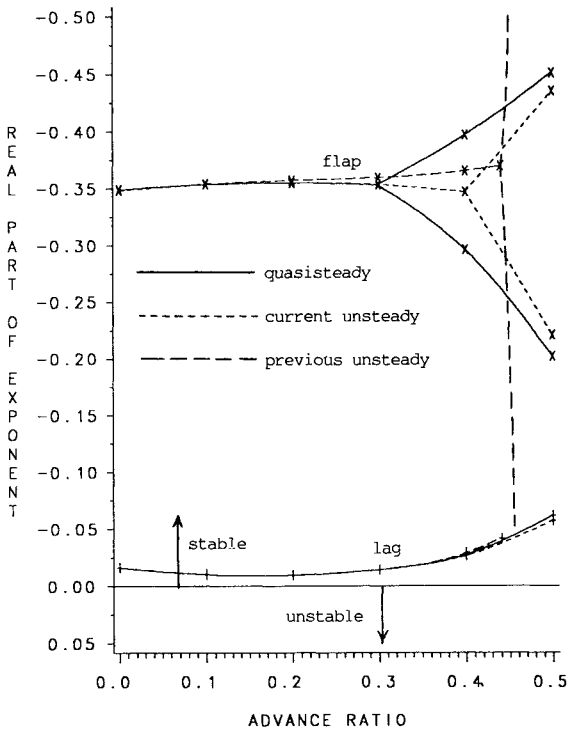

Fig. 5 Real part of characteristic exponent in flap and lag for quasisteady, previous unsteady, and current unsteady aerodynamic formulation, soft-in-plane blade.

standard soft-in-plane blade, for the torsionally stiff blade, and for the stiff-in-plane blade. The torsionally stiffer blade gave a tip response very similar to that shown in Ref. 10; whereas the torsionally softer blade gave the blade-tip response shown in Fig. 4. This was calculated at an advance ratio of 0.4 where the singularity in the air loads, discussed in the preceding section, has not yet greatly affected the tip response. The two formulations therefore give fairly similar results.

From the flap, lag, and torsional response for the soft-in-plane blade at an advance ratio of 0.4 presented in Fig. 4, it can be seen that unsteady effects produced only moderate differences in the flap and lag responses. The unsteady loads tend to lag behind the quasisteady loads due to the phase lag and amplitude modulation associated with the unsteady aerodynamics. The response of the stiff-in-plane blade was effected even less by the use of unsteady aerodynamics. As evident from Fig. 4, the influence of the time-domain, unsteady aerodynamics on the torsional response is more substantial. This is due in part to the inclusion of several higher-order apparent mass terms in the expressions for the aerodynamic momentum in the unsteady formulation, which were not included in the quasisteady formulation.

Stability results for the two torsional stiffnesses were quite similar. Plots of the variation with advance ratio of the real part of the characteristic exponent of the first-lag and first-flap modes for the standard soft-in-plane blade are given in Fig. 5. Data are plotted for the quasisteady, previous unsteady, and current unsteady aerodynamic formulations. It can be seen that the instability at an advance ratio of 0.45 noted in Ref. 10 does not occur when the problem is reformulated to avoid the singularity in the air loads.

The influence of time domain unsteady aerodynamics on the first-lag mode is very small. This is reasonable since the primary correction in the unsteady aerodynamic theory is to the lift. The influence of unsteadiness on the drag, which influences the lead-lag motion is small. There is however a noticeable effect of unsteady aerodynamics on the first-flap mode at higher advance ratios. Stability plots for the stiff-in-plane configuration are shown in Fig. 6. The first-lag mode instability characteristic of stiff-in-plane hingeless rotors in forward flight is apparent. Again the influence of the unsteady aerodynamics is small but increases with advance ratio.

The influence of unsteady aerodynamics on rotor response in the presence of high-frequency pitch excitations was investigated by applying a sinusoidal root pitch change $\Delta\theta$ of the form

$$\Delta\theta = A \sin(4\psi)$$

where the amplitude A was ⅓ deg. This root pitch change was superimposed on the collective trim value for the rotor. It should be emphasized that the zero phasing of this pitch change was completely arbitrary, and a different phasing would give very different values for the hub shears.

Figure 7 presents the variation of vertical shears with advance ratio for the soft-in-plane blade. Results are shown for both quasisteady and unsteady aerodynamics with and without such a high frequency pitch excitation. At higher advance ratios, the vertical shears without the pitch excitation show a large difference in magnitude, which depends on the type of aerodynamics used. The in-plane shears showed little difference between the two formulations. Again this is reasonable since the primary correction in the unsteady aerodynamic theory is to the lift, and the drag expression remains virtually unchanged.

In the presence of the high-frequency pitch excitation, there is some difference in vertical shears between the two models. At low advance ratios and at higher advance ratios, the difference becomes pronounced. The in-plane shears again showed little difference between the two aerodynamic formulations. With unsteady aerodynamics the 4/rev pitch excitation has a strong effect in relieving the 4/rev vertical hub shears. This effect is not captured using the quasisteady aerodynamics. It can be seen that at low advance ratios, where the values of the trim angles are small, the high-frequency pitch excitation merely increases the vertical shears by a fairly constant amount. This effect is probably due in a large part to inertial

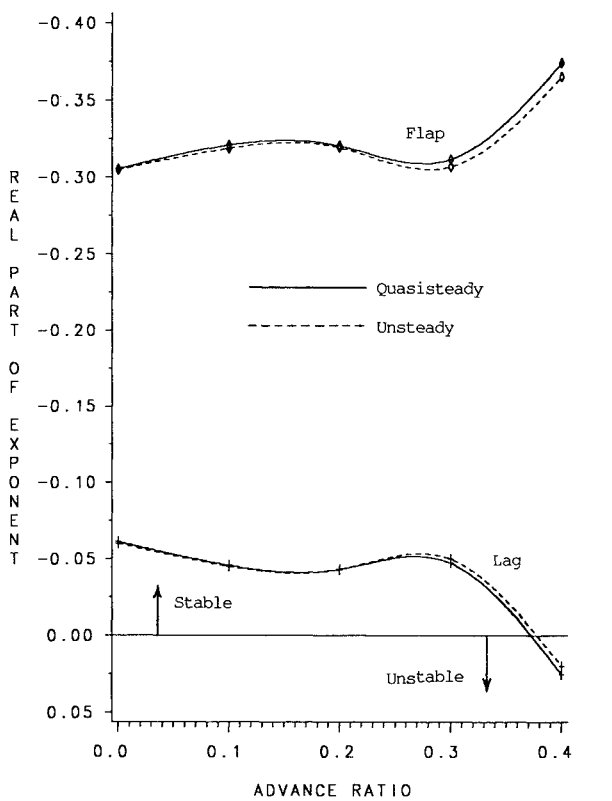

Fig. 6 Real part of characteristic exponent in flap and lag for quasisteady and unsteady aerodynamics, stiff-in-plane blade.

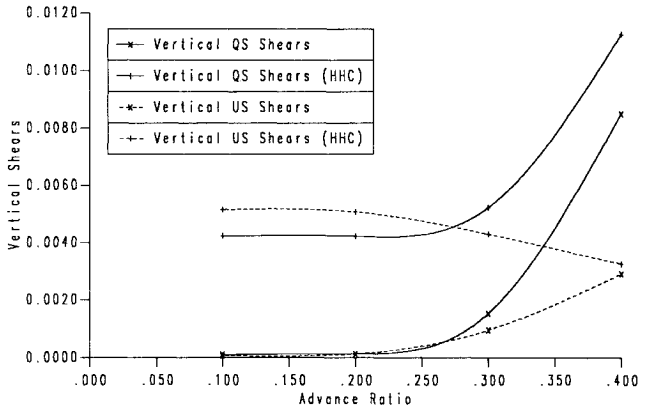

Fig. 7 Vertical shears vs advance ratio, quasisteady and unsteady aerodynamics, soft-in-plane blade, with and without 4/rev collective pitch excitation.

loads caused by the pitch change and is captured when either of the aerodynamic models is used. At higher advance ratios, however, the ability of the high-frequency pitch excitation to relieve the vertical shears is only captured by the unsteady aerodynamics.

Concluding Remarks

1) It has been shown that the instability in flap at high advance ratios found in Ref. 10 was not a result of the basic properties of the unsteady aerodynamics used nor was it due to the exclusion of the torsional degree of freedom in the aeroelastic analysis. The instability was caused by the specific choice of formulation in applying the unsteady aerodynamics to the aeroelastic analysis using the concept of a typical cross section. When a new implicit approach to formulating the air loads was implemented, using augmented states which vary along the blade span, the spurious singularity was eliminated.

2) It was found that the primary influence of unsteady aerodynamics is evident in the flap and torsional degrees of freedom. Overall differences in response with and without unsteady aerodynamics were small except at higher frequencies. The stability of the first flap mode was effected moderately at higher advance ratios by the inclusion of unsteady aerodynamics. This indicates that at low frequencies the effects of the wake for problems of this type are probably more important than the effects of unsteadiness. Development of aerodynamic models which can capture wake effects even approximately is therefore important. Furthermore it should be noted that compressibility and dynamic stall were neglected in this study; however these are known to produce important effects on rotor dynamics.

3) By observing the effect of quasisteady and unsteady aerodynamics on rotor hub shears in the presence of high-frequency pitch excitations, it was found that unsteady aerodynamics can have a significant influence on high-frequency components of the rotor response. This includes the capture of important hub-shear reduction effects due to pitch excitations, which are not apparent when quasisteady aerodynamics are used. This indicates that correct modeling of unsteady aerodynamic effects can be particularly important when analyzing the effects of higher harmonic control in reducing helicopter vibrations.

Acknowledgments

This research was supported by NASA Grants NAG 2-209 and NAG 2-477, funded by NASA Ames Research Center, Moffett Field, California. The comments of W. Wormbrodt and S. Jacklin are hereby gratefully acknowledged.

References

[1]Friedmann, P. P., "Formulation and Solution of Rotary-Wing Aeroelastic Stability and Response Problems," *Vertica,* Vol. 7, No. 2, 1983, pp. 101-141.

[2]Friedmann, P. P., "Recent Trends in Rotary-Wing Aeroelasticity," *Vertica,* Vol. 11, No. 1/2, 1987, pp. 139-170.

[3]Pitt, D. M., and Peters, D. A., "Theoretical Prediction of Dynamic Inflow Derivatives," *Vertica,* Vol. 5, No. 1, 1981, pp. 21-34.

[4]Goankar, G., and Peters, D., "Effectiveness of Current Dynamic-Inflow Models in Hover and in Forward Flight," *Journal of the American Helicopter Society,* Vol. 31, April 1986, pp. 47-57.

[5]Reddy, T. S. R., and Wormbrodt, W., "Forward Flight Aeroelastic Stability from Symbolically Generated Equations," *Journal of the American Helicopter Society,* Vol. 31, July 1986, pp. 35-44.

[6]Bir, G. S., and Chopra, I., "Gust Response of Hingeless Rotors," *Journal of the American Helicopter Society,* Vol. 31, April 1986, pp. 35-46.

[7]Nilakantan, G. H., and Gaonkar, G., "Feasibility of Simplifying Coupled Flap-lag-torsion Models for Rotor Blade Stability in Forward Flight," *Vertica,* Vol. 9, No. 3, 1985, pp. 241-256.

[8]Panda, B., and Chopra, I., "Flap-lag-torsion Stability in Forward Flight," *Journal of the American Helicopter Society,* Vol. 30, Oct. 1985, pp. 30-39.

[9]Friedmann, P. P., "Arbitrary Motion Unsteady Aerodynamics and Its Application to Rotary-Wing Aeroelasticity," *Journal of Fluids and Structures,* Vol. 1, No. 1, 1987, pp. 71-93.

[10]Dinyavari, M. A. H., and Friedmann, P. P., "Application of Time-Domain Unsteady Aerodynamics to Rotary-Wing Aeroelasticity," *AIAA Journal,* Vol. 24, No. 9, 1986, pp. 1424-1432.

[11]Dinyavari, M. A. H., "Unsteady Aerodynamics in Time and Frequency Domains for Finite-Time Arbitrary-Motion of Helicopter Rotor Blades in Hover and Forward Flight," Ph.D. Dissertation, Mechanical, Aerospace and Nuclear Engineering Dept., University of California, Los Angeles, March 1985.

[12]Shamie, J., and Friedmann, P., "Effect of Moderate Deflections on the Aeroelastic Stability of a Rotor Blade in Forward Flight," *Proceedings of the Third European Rotorcraft and Powered Lift Aircraft Forum,* Paper No. 24, Sept. 1977, pp. 24.1-24.37.

[13]Straub, F. K., and Friedmann, P. P., "Application of the Finite-Element Method to Rotary Wing Aeroelasticity," NASA CR-165854, Feb. 1982.

[14]Celi, R., and Friedmann, P. P., "Rotor Blade Aeroelasticity in Forward Flight with an Implicit Aerodynamic Formulation," *AIAA Journal,* Vol. 26, No. 12, 1988, pp. 1425-1433.

[15]Friedmann, P., and Kottapalli, S. B. R., "Coupled Flap-Lag-Torsional Dynamics of Hingeless Rotor Blades in Forward Flight," *Journal of the American Helicopter Society,* Vol. 27, Oct. 1982, pp. 28-36.